NASA/TM-20220007064

Repeatable Method for Conducting Chamber Studies of Aerosolized Lunar Simulant

Benjamin J. Sumlin
Universities Space Research Association, Cleveland, Ohio

Marit E. Meyer
Glenn Research Center, Cleveland, Ohio

December 2022

NASA STI Program . . . in Profile

Since its founding, NASA has been dedicated to the advancement of aeronautics and space science. The NASA Scientific and Technical Information (STI) Program plays a key part in helping NASA maintain this important role.

The NASA STI Program operates under the auspices of the Agency Chief Information Officer. It collects, organizes, provides for archiving, and disseminates NASA's STI. The NASA STI Program provides access to the NASA Technical Report Server—Registered (NTRS Reg) and NASA Technical Report Server—Public (NTRS) thus providing one of the largest collections of aeronautical and space science STI in the world. Results are published in both non-NASA channels and by NASA in the NASA STI Report Series, which includes the following report types:

- TECHNICAL PUBLICATION. Reports of completed research or a major significant phase of research that present the results of NASA programs and include extensive data or theoretical analysis. Includes compilations of significant scientific and technical data and information deemed to be of continuing reference value. NASA counter-part of peer-reviewed formal professional papers, but has less stringent limitations on manuscript length and extent of graphic presentations.

- TECHNICAL MEMORANDUM. Scientific and technical findings that are preliminary or of specialized interest, e.g., "quick-release" reports, working papers, and bibliographies that contain minimal annotation. Does not contain extensive analysis.

- CONTRACTOR REPORT. Scientific and technical findings by NASA-sponsored contractors and grantees.

- CONFERENCE PUBLICATION. Collected papers from scientific and technical conferences, symposia, seminars, or other meetings sponsored or co-sponsored by NASA.

- SPECIAL PUBLICATION. Scientific, technical, or historical information from NASA programs, projects, and missions, often concerned with subjects having substantial public interest.

- TECHNICAL TRANSLATION. English-language translations of foreign scientific and technical material pertinent to NASA's mission.

For more information about the NASA STI program, see the following:

- Access the NASA STI program home page at http://www.sti.nasa.gov

- E-mail your question to help@sti.nasa.gov

- Fax your question to the NASA STI Information Desk at 757-864-6500

- Telephone the NASA STI Information Desk at 757-864-9658

- Write to:
  NASA STI Program
  Mail Stop 148
  NASA Langley Research Center
  Hampton, VA 23681-2199

NASA/TM-20220007064

Repeatable Method for Conducting Chamber Studies of Aerosolized Lunar Simulant

Benjamin J. Sumlin
Universities Space Research Association, Cleveland, Ohio

Marit E. Meyer
Glenn Research Center, Cleveland, Ohio

National Aeronautics and
Space Administration

Glenn Research Center
Cleveland, Ohio 44135

December 2022

Level of Review: This material has been technically reviewed by technical management.

This report is available in electronic form at http://www.sti.nasa.gov/ and http://ntrs.nasa.gov/

Repeatable Method for Conducting Chamber Studies of Aerosolized Lunar Simulant

Benjamin J. Sumlin
Universities Space Research Association
Cleveland, Ohio 44135

Marit E. Meyer*
National Aeronautics and Space Administration
Glenn Research Center
Cleveland, Ohio 44135

Summary

To address the Agency's need to test spaceflight hardware in dusty environments, this report documents a method to generate an aerosolized mass concentration of lunar simulant using a specific combination of a Topas Solid Aerosol Generator (SAG) 410/U, Brechtel Model 9000 Passive Charge Neutralizer, and TSI DustTrak™ DRX (TSI, Inc.). An aerosolized mass concentration of 1.6 mg/m^3 was created and maintained for 2 hr, with the system automatically compensating for removal of dust by sampling and gravitational settling. This report also provides recommendations for constructing bespoke testing systems so that a variety of hardware may be tested.

Acronyms

ATD	Arizona Test Dust
DR	dosing ring
GASP	Gases and Aerosols from Smoldering Polymers
HEPA	high-efficiency particulate air
HLS	Human Landing System
ISO	International Standards Organization
LHS	Lunar Highlands Simulant
PID	proportional–integral–derivative
PM	particulate matter
PTFE	polytetrafluoroethylene
PV	process variable
RH	relative humidity
RFS	reservoir and feed screw
SAG	Solid Aerosol Generator
SP	setpoint
STD	standard
TPM	total particulate matter
USB	Universal Serial Bus

*Currently with Northrop Grumman.

Introduction and Motivation

The Artemis mission goal of returning humans to the Moon requires new solutions to engineering problems posed by the extremely harsh environment of the lunar surface. Using the Apollo missions as historical evidence, dust will be a significant obstacle in the success of a sustained human and robotic presence. Hardware such as tools, machinery, extravehicular activity suits, and components of landers and habitats will all be subject to various degrees of contamination by lunar dust, and each piece of hardware has its own considerations for performance under dusty conditions. Such hardware must be tested and verified for use during lunar missions under guidance from NASA technical standards. Aerosolized dust can be used to test and verify hardware in two ways: volumetric loading and surface area loading. Volumetric loading (measured in mass of airborne dust per volume of air) may cause hardware to malfunction via dust ingestion or other mechanisms. Surface area loading (measured in mass of settled dust per surface area) may cause hardware to malfunction by altering its thermal properties or by fouling optical surfaces such as camera lenses. This report describes a method to achieve a stable, user-determined volumetric loading in an arbitrary chamber along with recommendations for how to use such chambers for customized hardware testing.

The recent NASA Standard (STD) 1008, "Classifications and Requirements for Testing Systems and Hardware to be Exposed to Dust in Planetary Environments" (Ref. 1), defines four environments wherein dust is likely to be encountered and to pose significant risk to systems, derived from a matrix of the combinations of the presence of gravity (zero g or nonzero g) and the presence of an atmosphere (zero pressure or nonzero pressure). In pressurized environments, regardless of the presence of gravity, aerosolized dust has the potential to interfere with many systems and is most likely to cause contamination upon cabin ingress at the conclusion of an extravehicular activity.

Different space habitats have different requirements for the mass of dust per unit volume of cabin air (also known as mass concentration) that is permissible, typically as an average value over a given time period. These requirements are written in terms of PM_{10}, which is the mass concentration of all particulate matter (PM) with aerodynamic diameter of 10 μm or smaller, where aerodynamic diameter is defined as the diameter of a spherical particle with a material density of 1 g/cm^3 that has the same settling velocity as the particle in question. This metric necessarily requires one to consider the gaseous medium and flow field in which the particle is entrained, and, furthermore, invites discussion on the nature of the gravitational field and gaseous environment in which the analysis is taking place. Extended discussion of these factors is provided in Appendix A of this work and DeCarlo et al. (Ref. 2). For the purposes of this work, PM_X shall always be defined as the mass concentration of particles smaller than X μm, measured in Earth gravity at room temperature in air.

In the context of the Artemis Human Landing System (HLS) habitat, the requirements for PM_{10} are 1.6 mg/m^3 over 7 days, and 0.3 mg/m^3 over 6 months (Ref. 3). Defining this as an average value over a period of time allows brief, unavoidable spikes (e.g., the release of dust and other contaminants during routine crew activities like cleaning and vacuuming) to fall within specifications, provided they are rapidly remediated and the ambient dust concentrations remain low for the rest of the averaging period. This paper uses 1.6 mg/m^3 of total particulate matter (TPM) as an example target for a method to generate a consistent volumetric loading in a laboratory chamber with a volume of 0.33 m^3, suitable for testing and verification of small pieces of HLS hardware.

Another important measure of aerosolized material is the particle number concentration, which is the number of dust particles per unit volume of cabin air. Number concentration is not a requirement for HLS air quality; however, it is important to measure particle size distributions to fully contextualize the mass concentration. Typically, size-resolved measurements show that number concentration is dominated by smaller particles, whereas mass concentration is dominated by larger particles, because mass scales with

particle diameter cubed. In the context of Artemis requirements, PM_{10} will be dominated by particles near 10 μm, though the number concentration will be dominated by smaller particles. Instruments that measure number concentration, such as condensation particle counters, often do so with no discrimination of size and must be used in tandem with a size-resolving instrument. Furthermore, the literature often presents conflicting and subjective definitions of various size fractions, such as fine, ultrafine, respirable, thoracic, coarse, and so forth. To avoid the subjectivity associated with those terms, this work will only refer to specific fractions by their PM_X designations or by a specific diameter range in micrometers.

Aerosolization of a test material has a rich publication history, yet often the focus of such publications is either some sort of analysis on the aerosolized material itself, its interaction with or effects on the environment (e.g., climate and air quality research), or its industrial applications as a fabrication method (e.g., chemical vapor deposition). Recent work has demonstrated that there is a growing need for reliable and repeatable aerosolization methods for lunar dust simulant. For example, Vidwans et al. (Ref. 4) focus on the aerosolization of an older (yet popular) simulant, JSC–1A, which is no longer being manufactured. As the supply of available JSC–1A depletes, other simulants have been developed by NASA and other entities, such as universities and private companies. The technique herein may be applied to any dust simulant, though the results presented are for Lunar Highlands Simulant (LHS) 1D from Exolith Labs, an extension of the Center for Lunar and Asteroid Surface Science at the University of Central Florida. The technique follows the guidance specified in NASA–STD–1008, from preparation to storage and aerosolization (Ref. 1), and this paper serves to further contextualize and justify the great care that dealing with lunar simulants requires. Described here is a repeatable method to prepare and aerosolize an arbitrary simulant into any chamber. The equipment chosen and infrastructure needed are described in detail, and, where possible, alternatives are recommended. Four appendixes supplement the main text with discussions on equivalent diameters (Appendix A), proportional–integral–derivative (PID) controller tuning (Appendix B), instructions on how to clean the dust generator and change simulants (Appendix C), and the dust generator's electrical connector pinout (Appendix D).

Materials and Methodology

The following subsections describe the selection, preparation, and storage of lunar dust simulant; instrumentation; chamber and instrument setup; aerosolization control; and mass output calibration.

Simulant Selection

Lunar dust simulants are typically categorized based on their mineralogies and morphologies into "mare" and "highlands" simulants because they are engineered to represent those two regions. Mare regions are the darker regions of the lunar surface formed by ancient lava flows and can be expected to be predominantly basaltic. Highlands regions are brighter and predominantly anorthositic. This binary is largely sufficient to categorize lunar simulants, though it must be acknowledged that, for example, no highlands simulant will perfectly mimic every anorthositic region of the Moon. Beyond the Moon, martian simulants and those designed to mimic small bodies such as asteroids and comets can be quite varied. The Artemis III spacecraft is expected to land in the Moon's southern polar region, which is predominantly highlands. No single simulant is appropriate for all tests; however, this method is not specific to any one simulant. A lunar highlands simulant was chosen as the example for this paper.

Currently, many lunar simulants cataloged in the Colorado School of Mines Planetary Simulant Database (Ref. 5) are designated "available" or "may be available." Here, the aerosolization method was developed using LHS–1D and may be extended to any simulant. LHS–1 is composed of 74.4 percent anorthosite and 24.7 percent basalt by mass, with trace fractions of ilmenite, pyroxene, and olivine. In

particular, the LHS–1D size subset is specially prepared to contain only dust particles smaller than 30 μm in volume-equivalent diameter.

Volume-equivalent diameter is the volume of a sphere with the same volume as the particle in question. This parameter differs from the physical diameter of the actual dust particles because the typical dust particle is highly nonspherical (Refs. 2 and 6). Nonsphericity is parameterized in transport equations by the dynamic shape factor, which for terrestrial mineral dusts is often taken to be around 1.7 (Ref. 7). The choice to use volume-equivalent diameter, or any other equivalent diameter, is determined by the design of the instrumentation used to measure the dust particles. To simplify the mathematical treatment of an ensemble of irregularly shaped particles, the use of equivalent diameters is required, and the choice of equivalent diameter will depend on the instrument and physics involved. Volume-equivalent diameter is one of several equivalent diameters used in aerosol science. Another, the aerodynamic diameter, is often used by sampling equipment that analyzes the particles in situ, and is defined as the diameter of a spherical particle that has the same terminal velocity as the particle in question. For true spheres, all equivalent diameters are the same, and they diverge if particles are irregular. Irregularities are often parameterized by some shape factor that is applied to the entire population. A brief overview of volume-equivalent and aerodynamic diameters is given in Appendix A, along with discussion on the consequences of using equivalent diameters in exotic environments such as microgravity. This aerosolization method measures volumetric loading by aerodynamic diameter, which should be understood to be measured at room temperature, in air, on Earth.

Simulant Preparation and Storage

There are many considerations for simulant preparation to ensure the material best mimics expected behavior during a lunar mission, such as size fraction and moisture content. Sections 5.1.1 and 5.1.2 of NASA–STD–1008 (Ref. 1) provide guidance for how to best prepare a given simulant for testing. Further considerations are the electrostatic properties, such as the charge distribution. In this work, samples were stored sealed in a laboratory maintained below 20 percent relative humidity (RH) to prevent clumping, and the size selection (removing dust particles greater than 30 μm) was performed by the manufacturer.

When aerosolizing lunar dust simulants, preparation and use are a compromise between achieving the desired initial state of the simulant and maintaining that state throughout the test. The chamber itself should be representative of the expected mission environment as much as is practicable. At the time of writing, the target spacecraft cabin temperature and RH for the Artemis mission are still being determined, and so the aerosolization took place in a chamber at approximately 16 °C and 15 to 20 percent RH. Higher RH levels, such as aboard Gateway (design target nominally between 18 and 27 °C at between 25 to 75 percent RH (Ref. 3, Sec. 6.2.3.1)) have special considerations. Aerosolized dust is highly hydrophilic and will readily absorb available water vapor. This, in turn, will modify aerosol–aerosol and aerosol–environment interactions, which will affect the size distribution by increasing the rate of coagulation and other growth mechanisms (Ref. 8).

Instrumentation

Solid Aerosol Generator

Simulant was aerosolized by a Solid Aerosol Generator (SAG), model 410/U, Topas GmbH. This device utilizes a reservoir and feed screw (RFS) assembly and dosing ring (DR) mechanism to deliver dust to an aerosolizing nozzle. The rate of production is predominantly governed by controlling the rotation rates of the DR and RFS, which range from 0 to 100 in arbitrary units. The RFS rotation rate changes the amount of simulant deposited onto the DR, and the DR rotation rate changes how fast it moves simulant to the nozzle. Overall aerosol production is affected by parameters such as the distance of

the RFS disperser to the DR, the thickness of the DR (two rings are available, 0.3 or 1.0 mm; 0.3 mm was used here), the height of the nozzle from the DR, the input air pressure set by the external regulator, and the type of nozzle. (Three nozzles are available: 0.5 mm; 0.7 mm; and P-type, which is used to aerosolize fine powders that tend to clump.) In this work, these parameters are termed “external parameters” because they are external to the computerized control loop used here to control production rate. These external parameters are illustrated in Figure 1. In practice, these parameters were determined prior to experiments and held constant. Table I summarizes their values in this work. It is neither practical nor advised to alter these parameters during a test, nor can they be controlled remotely due to instrument limitations. Only the DR and RFS rates, here termed “internal parameters,” can (and should) be controlled remotely and dynamically. RFS was held constant at 30 to simplify the feedback control. Figure 2 shows a test powder (boehmite, Al(OH)O) staged on the DR as it travels to the nozzle.

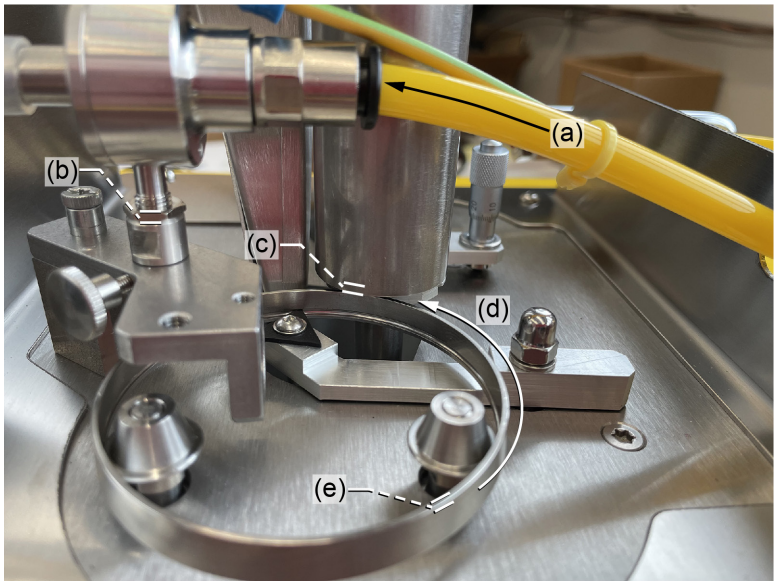

Figure 1.—Closeup of dosing mechanism showing various external parameters that control aerosolization rate. (a) Airflow. (b) Nozzle height. (c) Reservoir and feed screw (RFS) disperser to dosing ring (DR) distance. (d) DR rate. (e) DR thickness. RFS rate is obscured and not shown.

TABLE I.—SUMMARY OF EXTERNAL PARAMETERS (AND RFS) AND THEIR SETTINGS

Parameter	Effect and range	Value in this work
Distance of reservoir and feed screw (RFS) to dosing ring (DR)	Determines how much DR area is exposed to the simulant spray. Higher values correlate to a narrower spray area. Value is 0.00 to 5.00.	5
Thickness of DR	Determines how much simulant the DR can carry to the nozzle. Values are 0.3 or 1.0 mm.	0.3 mm
Nozzle height	Determines how effective the nozzle is at picking up simulant from the DR. (Closer is more effective.) Parameter has no values and is set empirically.	As close as possible
Inlet pressure	Determines both aerosolization efficacy and output flow rate. Values are 0 to 3 bar.	1.5 bar
RFS	Determines how much simulant is deposited on the DR. Values are 0 to 100 arbitrary units.	30

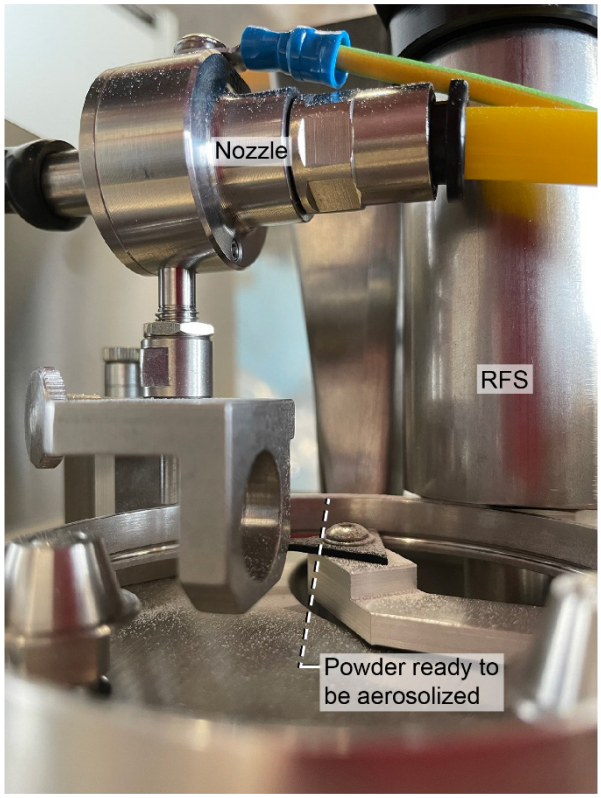

Figure 2.—Boehmite on dosing ring traveling to aerosolization nozzle. Reservoir and feed screw, RFS.

DR and RFS rates can be controlled from an external control unit plugged into the front of the SAG. In this work, a custom DB15 connector was constructed to connect to a data acquisition card (Universal Serial Bus (USB) 6008, National Instruments) that interfaces with the LabVIEW™ (National Instruments Corp.) graphical programming environment. The control program is described in the Aerosolization Control section of this document, and the DB15/USB–6008 connections are given in Appendix D (Table D.1).

The aerosolization mechanism is further enclosed in a methyl methacrylate chamber that has a filtered purge air tube attached. The purge air is supplied by the regulator and acts to balance the pressure in the mechanism one of two ways: (1) by balancing the purge air pressure below the nozzle pressure, an underpressure condition is created in the enclosure, preventing any aerosolized material from escaping to the surrounding environment; and (2) by balancing the purge air pressure above the nozzle pressure, an overpressure condition is created that prevents outside contaminants from intruding into the chamber. In this work, the SAG was located in a clean, vented enclosure and a slight underpressure condition was used to maintain safe working conditions as there was no risk of intruding contaminants. Lunar simulants contain a high amount of silica and thus pose a safety concern, so avoiding unsafe concentrations of respirable silica outside of the experimental setup must be prioritized. Figure 3 shows the pressure enclosure.

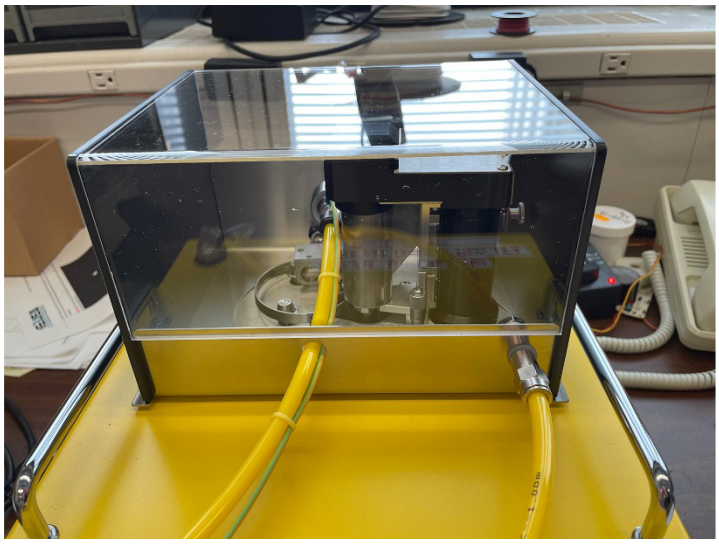

Figure 3.—Pressure enclosure supplied by nozzle airflow (left tube) and purge airflow (right tube).

DustTrak™ DRX

Aerosol concentrations were measured by a DustTrak™ DRX aerosol monitor (model 8534, TSI, Inc.; DRX hereafter), a scattering-based laser photometer that measures light scattering and derives values of 0.001 to 150 mg/m^3 in multiple size channels from PM_1 to PM_{10}, along with TPM, which is $PM_{10} + PM_{>10}$, where $PM_{>10}$ is approximately PM_{15} (Refs. 9 and 10). The measurement principle is based on light scattering by a narrowly focused aerosol stream, and the photometric response in the DRX is a combination of signals from a sophisticated photodetector: pulses from single particles and the photometric voltage signal. The algorithms used by the DRX, combined with some assumptions about the analyte, allocate the signal into PM_1, $PM_{2.5}$, PM_4, PM_{10}, and TPM. With a custom external software control program, additional features are available, such as size-resolved mass and number concentrations at 12 size bins derived from the photometric responses. Using these data, qualitative number and mass size distributions can be plotted, though these measurements are not officially sanctioned by the manufacturer. While the DRX is not a reference-quality instrument, it has a rich publication history and has been used in multiple NASA projects (Ref. 11).

The DRX is factory-calibrated to a reference instrument (TSI 8587 photometer, TSI, Inc.), which is itself calibrated to International Standards Organization (ISO) 121031 A1 test dust, also known as Arizona Test Dust (ATD) or Arizona Road Dust (Ref. 12). The photometric calibration is normalized to 1.0, and for dusts that differ greatly from ATD in mineralogy and/or morphology, a new multiplicative calibration constant must be determined for each simulant. This requires a colocated reference-quality mass measurement instrument or gravimetric sampler. Table II compares ATD with LHS–1D. ATD is compositionally similar to the LHS–1D simulant used in these tests, so the DRX calibration factor was left unchanged (Refs. 12 and 13).

This similarity does not extend to all simulants, however. For example, mare simulants tend to have a lower SiO_2 and higher MgO content, among other differences. As only the factory calibration is guaranteed by the DRX manufacturer, mare and other simulants should be calibrated for specifically.

Passive Charge Neutralizer

Because the aerosolization technique described later in this paper uses mechanical action to deliver dust to a flow stream, it is likely that some degree of tribocharging (charging due to mechanical

TABLE II.—COMPOSITION COMPARISON OF ATD AND LHS–1D

Component	Percent composition	
	ATD (Ref. 12)	LHS–1D (Ref. 13)
SiO_2	69 to 77	51.2
TiO_2	0 to 1	0.6
Al_2O_3	8 to 14	26.6
FeO	4 to 7	2.7
MnO	Not present	0.1
MgO	1 to 2	1.6
CaO	2.5 to 5.5	12.8
Na_2O	1 to 4	2.9
K_2O	2 to 5	0.5
P_2O_5	Not present	0.1

interaction) occurs. To mitigate this artifact, the aerosolized simulant is passed through a passive charge neutralizer (model 9000, Brechtel) equipped with a pair of 500-μCi (1.85×10^7 Bq) Po–210 sources (model 2U500, NRD, LLC). The neutralizer imparts a reproducible equilibrium charge distribution on an aerosol sample, mitigating wall, tubing, and sampling losses due to tribocharging. In this sense, the term "neutralize" refers to the process of neutralizing stray charges that go beyond $\pm1e$ to create a known charge distribution, rather than fully eliminating charges. Aerosol neutralized in this manner will still interact with the walls of the chamber in some way, but the effect is mitigated from the unneutralized state, where charge may accumulate on particles beyond $\pm1e$.

Chamber and Instrument Setup

The Gases and Aerosols from Smoldering Polymers (GASP) laboratory at Glenn houses a custom environmental chamber (hereafter referred to as "the chamber"), a repurposed 0.33-m^3 glovebox equipped with sample ports, digital communication lines, a recirculation fan, and a high-efficiency particulate air (HEPA)-filtered exhaust/cleanout system. The chamber also features a secondary containment structure and can be purged down to approximately 5 particles/cm^3 (virtually zero concentration). Most typical indoor spaces occupied by humans have ambient concentrations ranging from 1,000 to 10,000 particles/cm^3 (Ref. 14). The chamber is suitable for testing at ambient pressure and temperature. The SAG is connected through the neutralizer and into the rear of the chamber via short lengths of conductive silicone rubber tubing to minimize tubing losses due to gravitational settling, inertial deposition, and electrical migration (Ref. 8). Other options for tubing are copper, stainless steel, or conductive polytetrafluoroethylene (PTFE). The tubing material is not strictly the most important parameter; its electrical conductivity is. It is vital that the tubing be electrically conductive to eliminate static electricity buildup due to friction between the tube and its moving contents. The DRX is connected to the chamber (also with conductive tubing) through a sampling port on the side of the chamber. Inside the chamber, the SAG and DRX connections intrude approximately 8 in. into the central volume and are held in place by tube clamps mounted on a titration stand. The recirculation fan is oriented away from both tubes to create a gentle air current for mixing the volume without directly affecting generation or sampling.

Figure 4 shows the exterior of the chamber with all instrumentation, and Figure 5 shows the orientation of the sampling tubes on the titration stand. All conductive tubing is electrically connected to the chamber's metal frame, which in turn is connected to the building's electrical earth connection, further mitigating tubing losses.

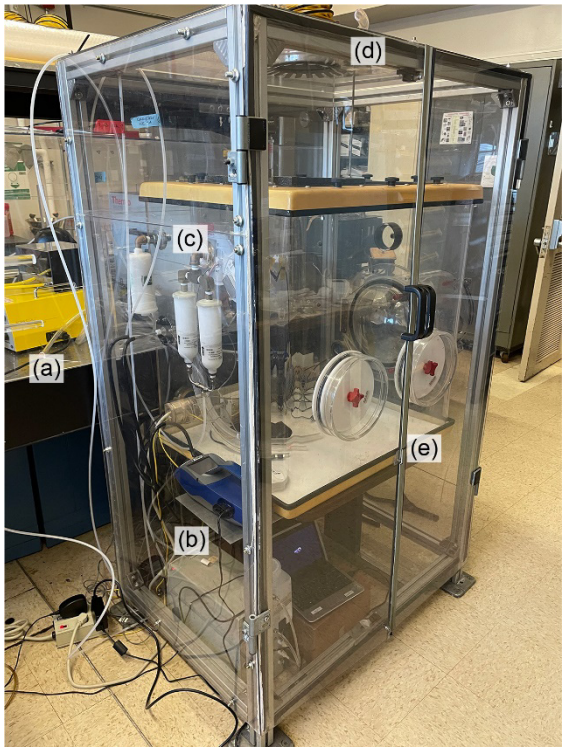

Figure 4.—Double-enclosed glovebox chamber in Gases and Aerosols from Smoldering Polymers (GASP) laboratory at NASA Glenn Research Center. (a) SAG 410/U. (b) DustTrak™ DRX. (c) HEPA-filtered purge system. (d) Building ventilation. (e) Glovebox ports.

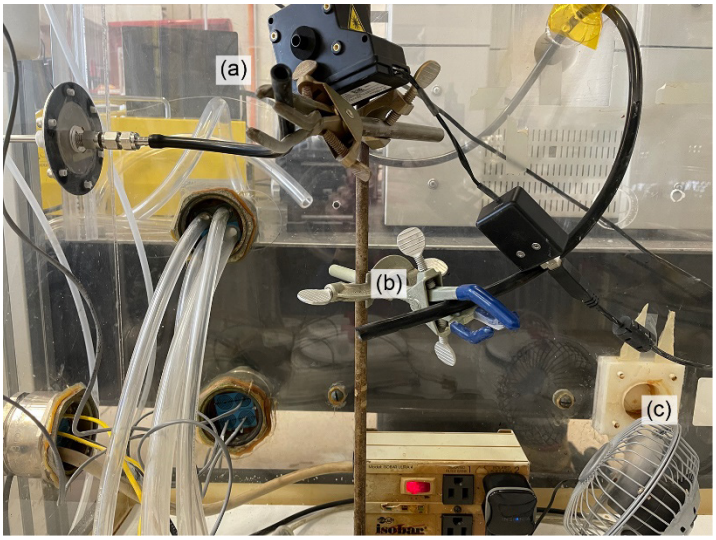

Figure 5.—Chamber setup. (a) Sample tube. (b) Supply tube. (c) Circulation fan.

Aerosolization Control and Mass Output Calibration

The SAG and DRX are controlled from a custom program written in LabVIEW™ 2020 software (National Instruments Corp.). The program can either control the SAG manually by allowing the user to input DR and RFS rotation rates using a full-range scale (0 to 100, arbitrary units), or it can use a PID controller to automatically adjust the DR (given a constant RFS rate) to create a user-specified mass concentration (mg/m^3) measured in PM_1, $PM_{2.5}$, PM_4, PM_{10}, or TPM. Note that this does not mean that the chosen size fraction is all that will be present in the chamber, only that the system will use the measurement of that size fraction to control aerosol production. The tuning of the PID controller can be a time-consuming process, though standard algorithms like Ziegler–Nichols can provide an excellent starting point. The PID system and the tuning process are briefly discussed in Appendix C, and the tuning process should be applied to any new chamber, or when the internal geometry changes significantly due to the presence of a large piece of test hardware.

The combination of the low dose rate of the SAG 410/U, the tendency of simulants to clump, and a large chamber volume to fill leave this system prone to measurement noise and considerable dead time. However, with appropriate care in simulant preparation, chamber configuration, and digital measurement filtering, these issues can be overcome.

Simulant Aerosolization Challenges

An ideal substance to be aerosolized would not adhere to itself (clumping), would be effortlessly and evenly deposited onto the DR by the RFS, and would be entirely aerosolized by the SAG nozzle. Unfortunately, when using simulants, none of these ideal assumptions hold true. Figure 6 illustrates the locations in the SAG where these issues occur. The result is that simulant does not steadily move to the nozzle; rather, it arrives at the nozzle in discrete chunks that are then aerosolized in pulses. This artifact can be somewhat mitigated by overspraying the DR, which is accomplished by setting a high RFS rate. However, overspraying interacts with the clumping problem, where large clumps may inadvertently knock simulant off the DR, and even when simulant does land correctly, it is still not evenly dispersed. Fortunately, the shear force of the nozzle is enough to break up large clumps almost entirely. The greatest mitigating factor to the uneven dispersion issue is the large volume of the chamber and appropriate mixing using the recirculation fan. As seen in Figure 5, though the inlet and outlet tubes in the chamber seem close, they are oriented in different directions such that the dust has enough time to evenly distribute in the chamber and satisfy the assumption that the DRX is sampling thoroughly mixed air. The result is that one may assume the chamber to be well mixed, and the only noise in the measurements is the noise from the DRX. At a maximum, the DRX reports data at 1 Hz, though smoothing may be applied or longer time periods may be averaged together. In these tests, however, measurement noise was not a large factor, so the native 1-Hz data are reported.

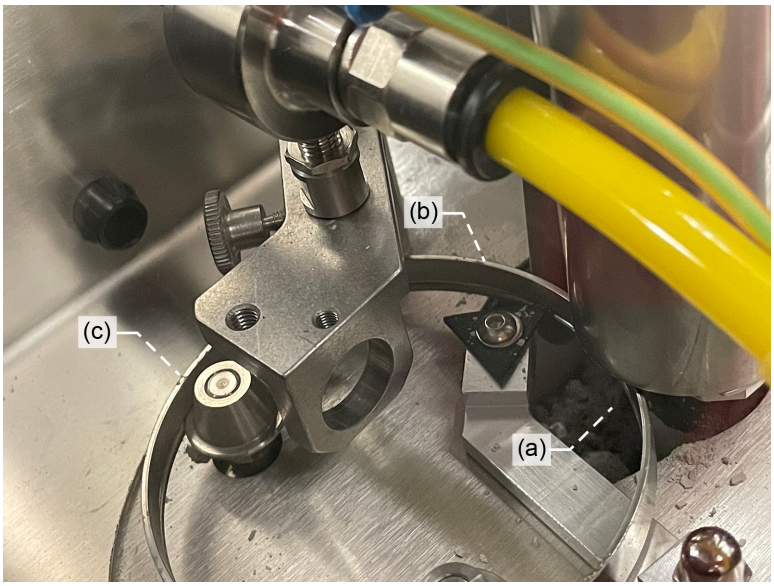

Figure 6.—Simulant aerosolization challenges in Solid Aerosol Generator (SAG). (a) Clumped simulant in reservoir. (b) Tiny packets of simulant rather than continuous, even dose. (c) Leftover simulant not captured by nozzle.

Manual Control and Calibration

In the event that the SAG is to be controlled manually, it must be calibrated for mass output for every simulant used. This calibration can be done in two ways. The preferred method is to aerosolize simulant in a chamber where it is collected by a filter sampler for gravimetric analysis. Several filters are required so that several data points are collected, and this process is prone to errors and artifacts. First, an appropriate filter sampling setup must be designed that includes the filter holder (e.g., MilliporeSigma model XX5004700), flow control valve, and a vacuum pump, such that flow rates through the filter are precisely controlled. Second, an appropriate microbalance capable of microgram resolution is needed, and it should have a radioactive source to neutralize stray charges on the filters. Filters must be preweighed, baked at 900 °C (Ref. 15, Sec. 9.11), and stored in a sealed petri dish. For each filter, the DR setpoint is held constant. Dust is sampled onto the filter for a set amount of time, after which the filter is weighed. Repeating this process at multiple DR setpoints, a scatter plot of mass per time can be constructed using the mass deposited on the filter and the time it took to deposit it. The transfer function between DR rate and mass output per unit time is linear, and the slope and offset of a linear regression line can be used to calibrate any DR setpoint to a desired mass output per unit time. Again, these calibration factors are not required when using external control software that simultaneously monitors aerosolized mass concentrations because the control algorithm accounts for the transfer function. Furthermore, because there is no way to input the calibration factors into the SAG itself, one must calculate the calibration by hand or generate a lookup table. It is recommended that external control be used.

The second method uses online analysis from the DRX (or any online instrument that reports mass concentration). A time series is gathered using multiple DR setpoints. The TPM data is numerically integrated over the time interval corresponding to a given DR setpoint and divided by the length of the interval. This result is multiplied by the DRX flow rate to obtain a mass output per unit time corresponding to various DR setpoints, and a linear regression can be performed as with the offline method. This online method is not recommended because it is highly susceptible to the aerosolization issues described in the previous section and requires a careful arrangement of the SAG, DRX, and a pressure relief filter. However,

this method may be used in cases where gravimetric analysis or external SAG control is not possible. The flow rate out of the SAG and into the DRX must be known and can be estimated from Figure 7.

In this case, the SAG was equipped with a P-type nozzle and its inlet pressure was set at 1.5 bar. This setting correlates to an output airflow rate of 0.035 l/min[1] (Figure 7) while the DRX was sampling at 3.0 l/min[1]; therefore, 98.2 percent of the air sampled by the DRX was clean makeup air. The calibration setup is shown in Figure 8, and the result of the calibration by this method is shown in Figure 9. To apply this calibration in practice, a sample table of input and output values for LHS–1D is given in Table III. The final entry in the table, 41.3 µg/s[1], is the maximum rate available under this calibration.

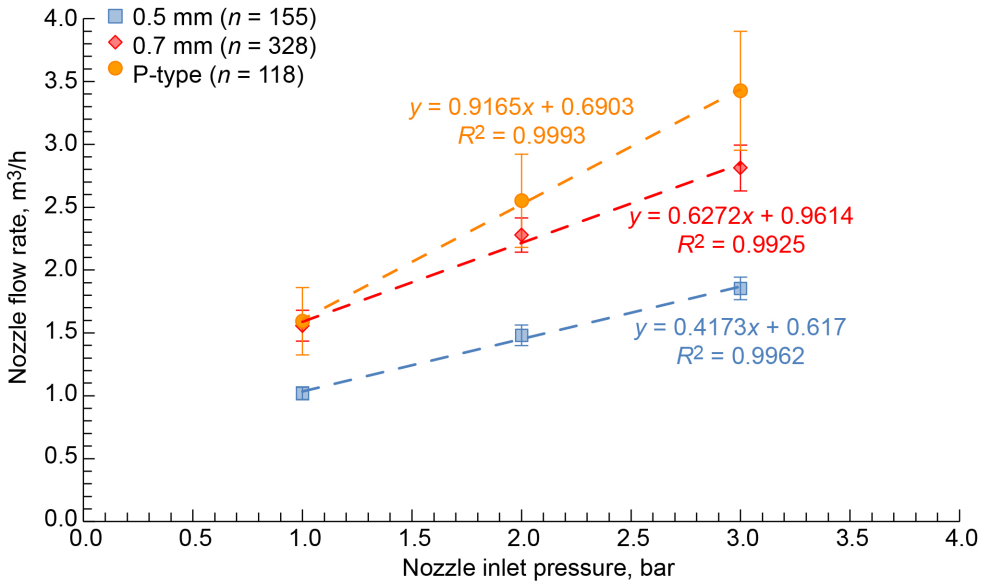

Figure 7.—Characterization of three SAG 410/U nozzles: 0.5 mm, 0.7 mm, and P-type (used in this work). Adapted from graph provided by Topas; used with permission. Number of data points, *n*.

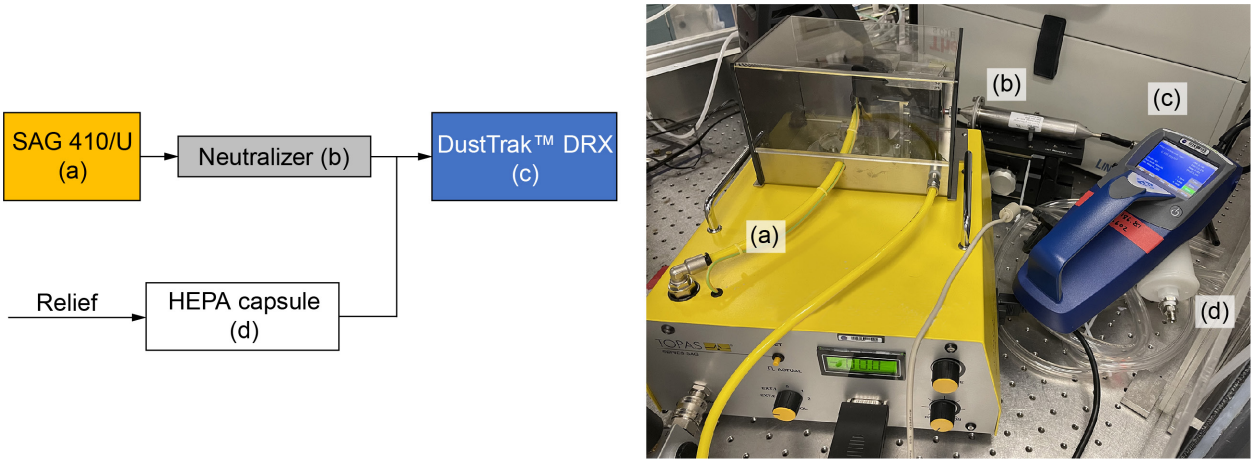

Figure 8.—Setup for online calibration. (a) SAG. (b) Neutralizer. (c) DRX. (d) HEPA-filter capsule for pressure relief.

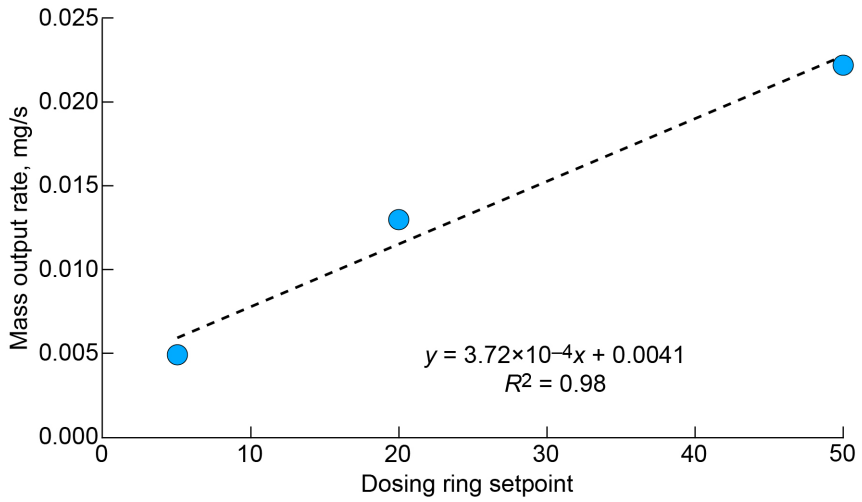

Figure 9.—Three-point calibration curve for mass flow rate as function of dosing ring rotation rate, corrected for SAG and DRX flow rates. This calibration uses reservoir and feed screw (RFS) rate of 30 and P-type nozzle at 1.5 bars inlet pressure aerosolizing LHS–1D.

TABLE III.—VARIOUS MASS FLOW RATE SETPOINTS AND THEIR CORRESPONDING DOSING RING SETPOINTS
[Derived from calibration shown in Figure 9.]

Mass output rate (μg/s[1])	Dosing ring setpoint
5.0	2.5
10.0	15.9
15.0	29.4
20.0	42.8
25.0	56.2
41.3	100 (maximum)

Results, Discussion, and Recommendations

Mass Concentration, Number Concentration, and Size Distribution Over Time

A time series for a TPM setpoint of 1.6 mg/m^3 is shown in Figure 10. From the time the TPM concentration (purple trace) crosses the setpoint to the time the test ends, the average mass concentration within the chamber was 1.67±0.11 mg/m^3. The overshoot can be attributed to a nonideal PID controller gain setting, which is discussed in subsequent sections. Smoothing the data with a moving average low-pass filter (green trace) reduces the measurement error to ±0.08 mg/m^3.

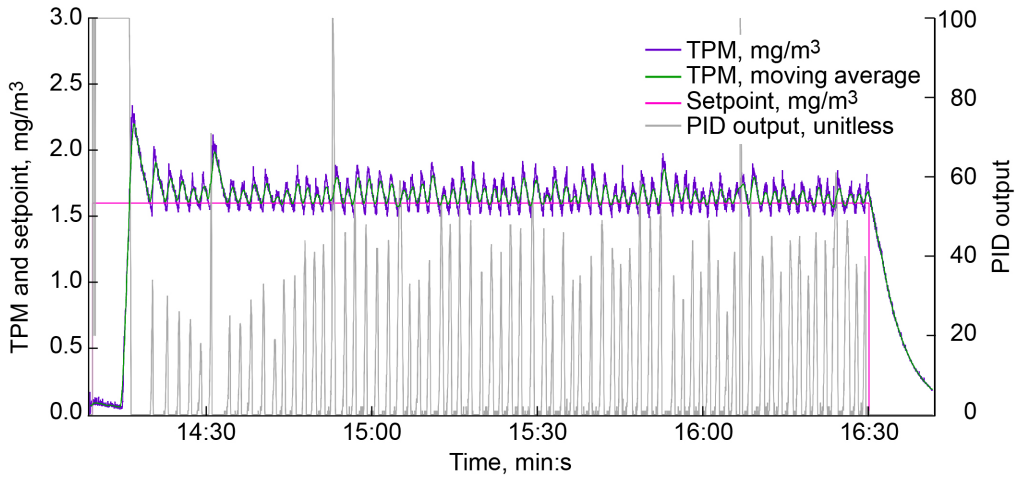

Figure 10.—Results from using naïve, untuned PID controller to control volumetric concentration.

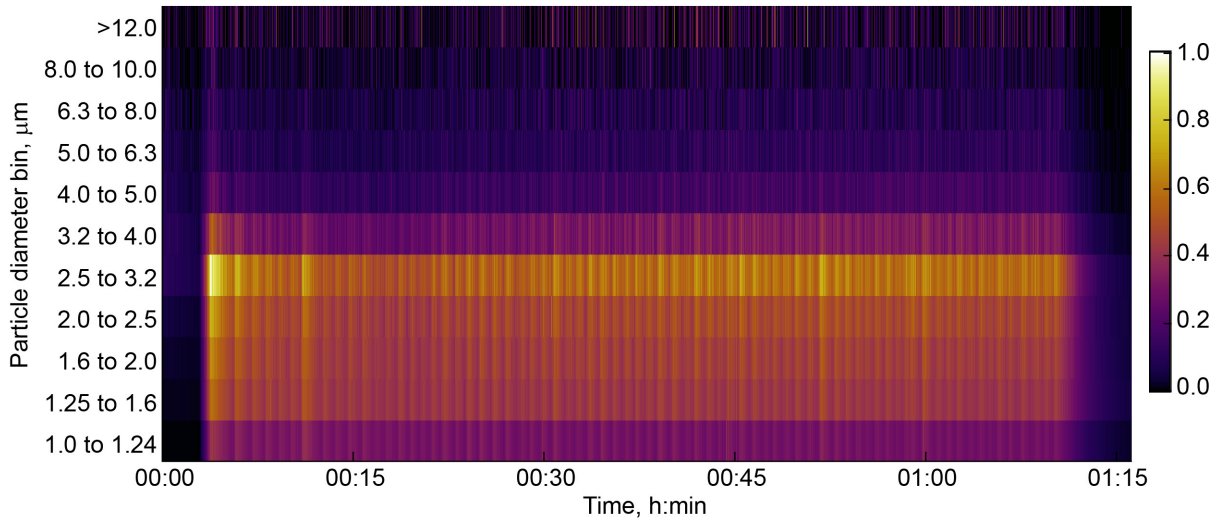

Figure 11.—Normalized mass concentration across experiment time, omitting <1-µm bin.

The TPM concentration time series can be further investigated by looking at the mass and number size distribution evolution along the experiment time. However, plotting these size distributions can be confounded by the inclusion of the smallest bin (particles 1 µm and smaller) reported by the DRX's extra features, because over time it can be expected that smaller particles will remain in the chamber while larger particles settle out due to gravity. Some particles will migrate to the walls of the chamber, but this is mitigated by neutralizing the charge distribution (as described earlier) and relying on the fluid boundary layer to keep particles entrained and following streamlines. The mass concentration size distributions without the smallest bin are plotted in Figure 11, followed by the number distributions in Figure 12. Figure 13 shows five size distributions taken from evenly spaced time steps of the mass concentration time series at 0:15, 0:30, 0:45, 1:00, and 1:15 after experiment start. When dust is present, the measured size distribution shows a mode diameter between 2.5 and 3.2 µm. The data are normalized to the maximum value in each data set because the multichannel methods have not been established for all types of aerosol, and these data are largely qualitative.

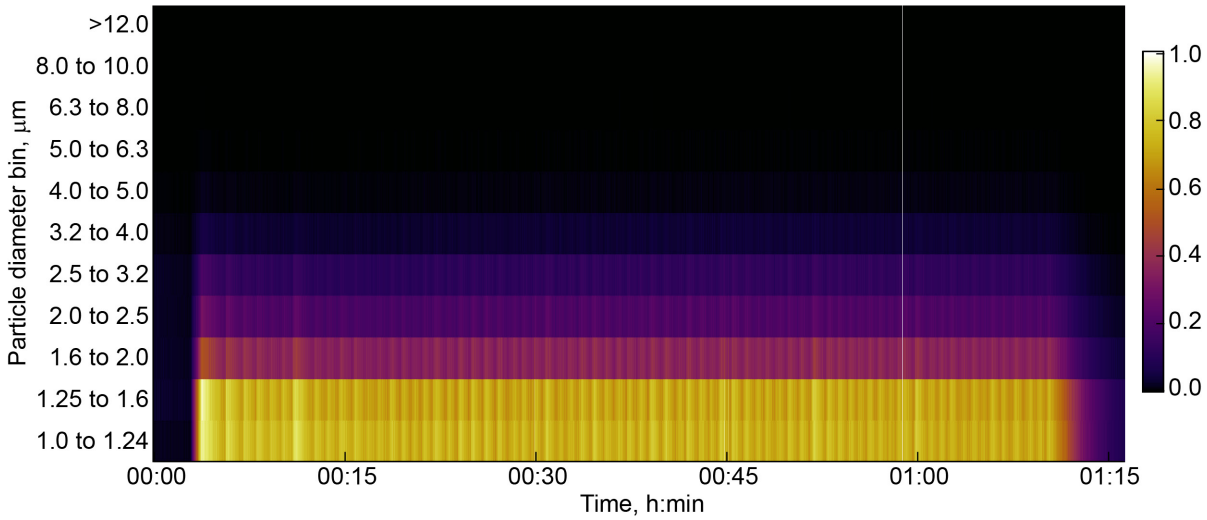

Figure 12.—Normalized number concentration across experiment time, omitting <1 μm bin. Note that smaller particles still dominate system.

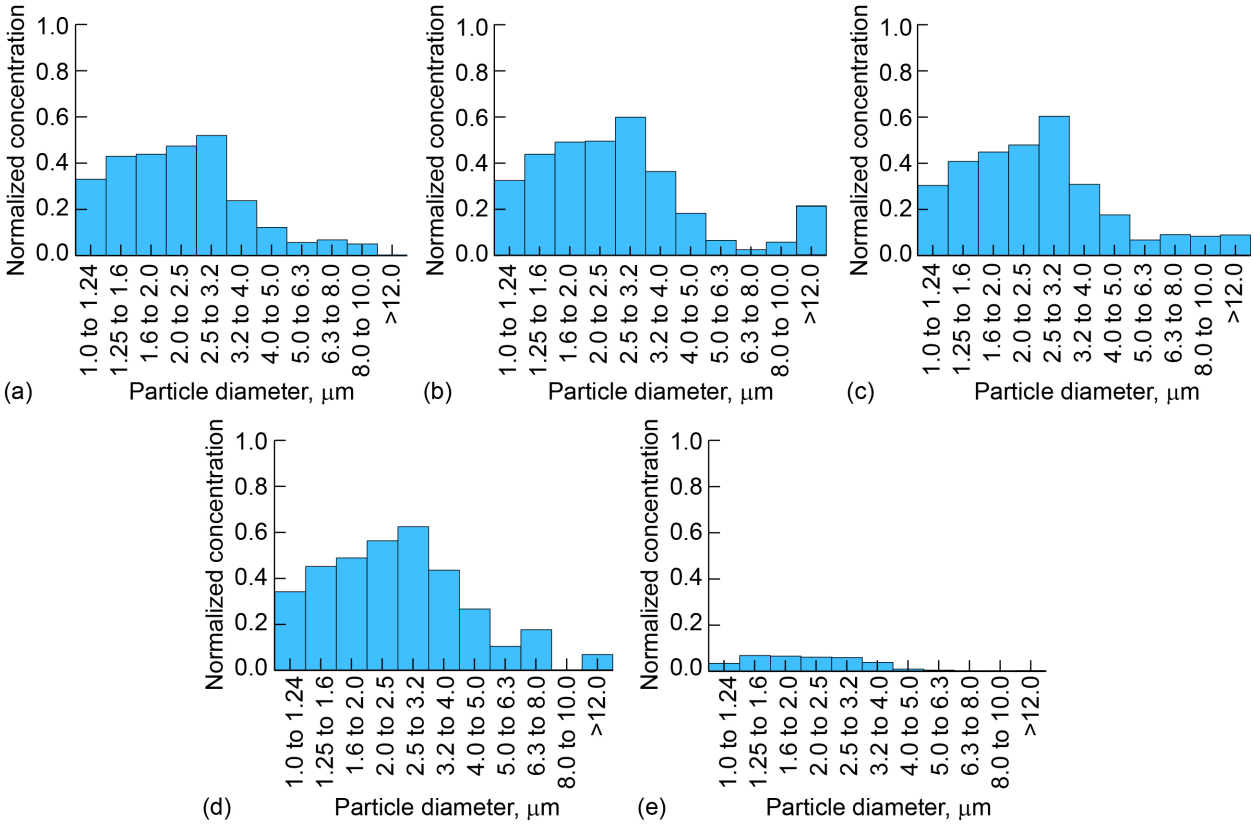

Figure 13.—Five size distributions taken from 15-min intervals across the experiment timeline. (a) 15 min. (b) 30 min. (c) 45 min. (d) 60 min. (e) 75 min.

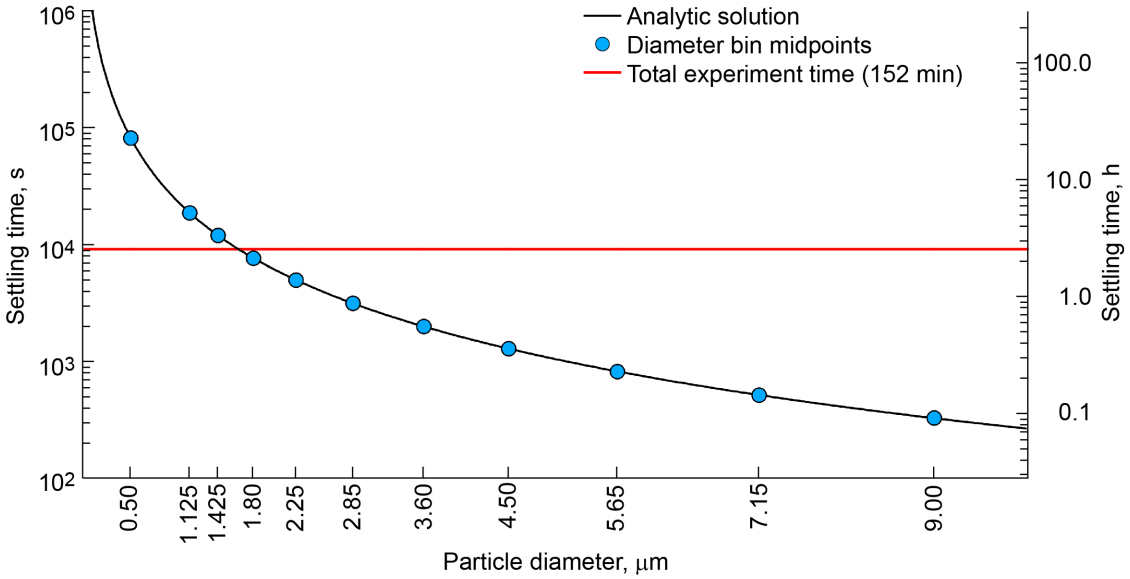

Figure 14.—Plot of calculated average settling times in a 0.6-m-tall chamber across the DRX size spectrum (black line) with DRX extra data bin midpoints plotted individually (blue circles). Total experiment time shown in red for reference.

When measuring aerosolized simulant, the settling time of the material in the chamber must be considered. Figure 11 and Figure 12 can be further contextualized with Figure 14, which is a plot of the theoretical average settling time of LHS–1D in an 0.6-m-tall chamber, assuming the chamber is well mixed yet perfectly still and without additional input (Ref. 16). This graph essentially shows a baseline calculation without the effects of the recirculation fan and the continuous generation of dust from the SAG. These baseline calculations are a useful illustration of the effects of gravitational settling, but the recirculation fan and continuous generation complicate the calculations of the actual retention within the chamber. The x-axis shows the midpoint of the bins at which the DRX measures, and the red line shows the total experiment time. Particles smaller than 1.425 μm can be expected to remain aloft for longer than the duration of the experiment, and therefore it stands to reason that they will accumulate within the chamber. This is a necessary consideration not only for hardware testing, but for mission design itself. The presence of small particles may evade any standards based on PM_{10}, because while small particles contribute vanishingly to total mass, they dominate by number.

Discussion

To analyze the dynamics of the system in the chamber, we begin by describing it with a mass balance equation:

$$Accumulation = Input - Output + Generation - Consumption$$

where *Accumulation* is the rate of change of the mass concentration within the chamber, *Input* is the mass concentration rate of change due to aerosolized dust, and *Output* is the removal rate by sampling instruments. We assume no creation of additional dust within the chamber, nor resuspension of settled dust by the recirculation fan, so *Generation* is zero. The *Consumption* term, however, is useful and interesting. Consumption within this system occurs by two methods: gravitational settling and wall losses. The PID system, by measuring only concentration, removes the need to strictly compute for consumption in the system. Consumption is difficult to compute because the recirculation fan (1) prevents dust from

settling and (2) drives it to walls, though this is mitigated by the formation of a fluid boundary layer. The flow remains gentle enough such that most dust particles remain Stokesian, that is, particles still tend to follow the streamlines of the gas flow field (Ref. 8). However, gravitational settling may be a useful method for studying the effects of dust on hardware that will be subject to such phenomena (e.g., any hardware located on or near the floor of a pressurized habitat). Over time, despite airflow from the recirculation fan, dust will settle. This method can be used for testing hardware exposed to surface area loading by deposition, though there are applications using mechanical sieving that can deposit a controlled amount of dust on a surface, both in pressurized and vacuum environments.

Tuning the Chamber for Hardware Experiments

Any change to the geometry of the chamber, such as installing or removing a piece of hardware to be tested, will likely require a retuning of the PID gain parameters. It is recommended that this be performed with a protected (e.g., wrapped in plastic) piece of hardware installed in the chamber. A piece of hardware whose physical extents occupy no more than approximately 10 to 20 percent of the chamber volume (0.07 to 0.13 m^3) should not require retuning.

Conclusions

This report documents a method to generate an aerosolized mass concentration of lunar simulant using a specific combination of a Topas Solid Aerosol Generator (SAG) 410/U, Brechtel Model 9000 Passive Charge Neutralizer, and TSI DustTrak™ DRX aerosol monitor. These are not the only options for instrumentation; however, the complexities of aerosolization and closed-loop control require that any instruments chosen have a few necessary features. For example, any dust disperser should have an option for external control via custom programming, and any aerosol measurement should report mass concentration. Using an instrument that only reports number concentration, for example, would be inappropriate to conduct testing against NASA spacecraft cabin air quality requirements. It is recommended that researchers obtain input from subject matter experts in the field of aerosol science and technology before constructing a custom setup.

Appendix A.—Equivalent Diameters

A.1 Problem of Aerodynamic Diameter

Start with Equation (A.1) for terminal settling velocity (V_{TS}), which is a function of the aerodynamic diameter d_a, gas density ρ_0, gravitational acceleration g, and gas kinematic viscosity η. Equations (A.2.a) and (A.2.b) introduce subscripts E and M for Earth and Moon, respectively. Equation (A.3) relates lunar and Earth gravity.

To find the relationship between aerodynamic diameters on the Moon and Earth, start by setting their terminal velocities equal, as in Equation (A.4). Substitute Equation (A.2) to get Equation (A.5). Simplify to get Equation (A.6). Substitute Equation (A.3) to get Equation (A.7). Solve for $d_{a,E}$ to get Equation (A.8).

Because aerodynamic diameter is the length scale by which PM_X (mass concentration of particles smaller than X μm) is defined, PM_X on the Moon will be a factor of $\sqrt{6}$ larger than on Earth. Furthermore, by this commonly accepted definition, it makes little sense to talk about PM_X in zero gravity, such as on the International Space Station, and PM_X in a vacuum is entirely meaningless unless one explicitly states that it is measured with the vacuum aerodynamic diameter. Finally, in different pressure environments (such as the reduced pressure aboard the Human Landing System), the aerodynamic diameter will change not only according to gravity, but also according to the gas density ρ_0.

$$V_{TS} = \frac{\rho_0 d_a^2 g}{18\eta} \tag{A.1}$$

$$V_{TS,E} = \frac{\rho_0 d_{a,E}^2 g_E}{18\eta} \tag{A.2.a}$$

$$V_{TS,M} = \frac{\rho_0 d_{a,M}^2 g_M}{18\eta} \tag{A.2.b}$$

$$g_M = \frac{1}{6} g_E \tag{A.3}$$

$$V_{TS,E} = V_{TS,M} \tag{A.4}$$

$$\frac{\rho_0 d_{a,E}^2 g_E}{18\eta} = \frac{\rho_0 d_{a,M}^2 g_M}{18\eta} \tag{A.5}$$

$$d_{a,E}^2 g_E = d_{a,M}^2 g_M \tag{A.6}$$

$$d_{a,E}^2 g_E = \frac{d_{a,M}^2 g_E}{6} \tag{A.7}$$

$$d_{a,E} = \frac{1}{\sqrt{6}} d_{a,M} \text{ or } \sqrt{6} d_{a,E} = d_{a,M} \tag{A.8}$$

This factor of $\sqrt{6}$ has important implications in the treatment of airborne particles in low-gravity and/or low-pressure environments because there is a discrepancy between the sampling and optical mechanisms in a measurement instrument. Sampling mechanisms, such as size-selective inlets, rely on

certain assumptions to correctly sample a given d_a size fraction, and these assumptions generally hold in all nonexotic terrestrial environments. Aerosol light scattering behavior is unaffected by these variables provided the refractive index of the gaseous medium is close to unity (e.g., in air). These assumptions further extend to the human respiratory system, which acts as a staged impactor, where different PM fractions have different penetration depths into the body. For example, larger particles (e.g., particles with $d_a \geq 10$ um) deposit in the upper respiratory system, whereas the smallest particles (e.g., $d_a \leq 1$ um) can deposit in the alveoli, where toxicants can transfer directly into the bloodstream. Inaccurate mass concentration and particle size distribution measurements could have health-threatening implications for future space exploration. From Equation (A.8), an instrument that measures PM_{10} on the Moon would measure $PM_{24.5}$ on Earth. Conversely, an instrument that measures PM_{10} on Earth will, at best, measure $PM_{4.1}$ on the Moon, even neglecting necessary modifications due to reduced pressure. Uncorrected instruments will fail to measure a large portion of the particulate mass that can have detrimental effects in the human body and will not satisfy requirements that are written in terms of PM_{10}.

Appendix B.—Control Loop Tuning

B.1 Tuning PID Settings

A proportional–integral–derivative (PID) control loop is a common tool in industrial process engineering to control a system while simultaneously measuring a variable of interest (the process variable, or PV)—for example, controlling a heating system while measuring a thermocouple. These control loops are often used when the system has a variable that must respond quickly to changes in the process setpoint (SP) without fluctuations such as overshooting or undershooting, or oscillations around the SP. The control function is written as

$$u(t) = K_C e(t) + \frac{K_C}{T_I}\int_0^t e(\tau)\,dt + K_C T_D \frac{de(t)}{dt} \tag{B.1}$$

where $u(t)$ is the controller output, K_C is the proportional gain constant, T_I is the integral time constant, T_D is the derivative time constant, and $e(t)$ is the error term, which is the difference between the SP and the PV. Some implementations of this equation replace K_C/T_I with K_D and $K_C T_D$ with K_D. "Tuning" refers to the process of determining the appropriate values of these coefficients for a given system.

A PID controller responds to the error term by increasing the controller output. In this work, the SP was 1.6 mg/m^3 and the PV was total particulate mass (TPM) measured by the DustTrak™ DRX aerosol monitor. The time series for the system without PID tuning using only default values of $K_C = 1$, $T_I = 0$ (which, in the algorithm, sets the entire integral term to zero rather than diverging to infinity), and $T_D = 0$ is shown in Figure 10. Even without tuning, in this system the PID controller can achieve and maintain values around the 1.6 mg/m^3 SP, which is close to the PM_{10} requirements for the Human Landing System. From the time the mass concentration in the chamber first crossed the SP to the end of the test, the average concentration in the chamber was 1.67±0.11 mg/m^3. The overshoot is a result of the process dead time and can be corrected for by using a nonzero T_D.

A simple tuning method is the Ziegler–Nichols tuning algorithm (Ref. 17), a heuristic algorithm that begins by setting T_I and T_D to zero and manipulating only K_C until the PV reaches a stable oscillation around the SP. This gain is denoted K_O. The oscillation time period T_O is then measured (in minutes). From K_O and T_O, the PID parameters are calculated as $K_C = K_O/5$, $T_I = T_O/2$, and $T_D = T_O/3$. Here, T_O is 121 s, or 2.07 min. From this K_O and T_O, the coefficients are $K_C = 0.2$, $T_I = 1.035$, and $T_D = 0.69$.

The moving average low-pass filter permits an easier calculation of the oscillation period and reduces the standard deviation of the average slightly, though the actual average remains unchanged within measurement uncertainty. This is a testament to the robust measurements provided by the DRX.

Ziegler–Nichols is not the only algorithm to calculate PID gains from dead time. For some systems prone to large oscillations, the Tyreus–Luyben coefficients (Ref. 18), which are used in the same heuristic process as Ziegler–Nichols, may be a better choice. This may help for larger chambers where the dead time is significant, or when using dust dispersers that are capable of larger output per unit time than the SAG 410/U used here.

Appendix C.—Procedure for Changing Simulants

This appendix documents a procedure for removing unused simulant from the Topas Solid Aerosol Generator (SAG) 410/U, cleaning the instrument, and loading new simulant. This procedure should be performed each time a new simulant is to be aerosolized, at a minimum. Depending on the relative humidity in the laboratory where the work is being performed, simulant may need to be changed more frequently, as it takes up water while sitting in the SAG reservoir. Unused simulant can be reused, provided it is fully baked out according to NASA–STD–1008, Sec. 5.1.2 (Ref. 1).

This procedure requires the following tools and materials: T15 driver, lint-free disposable towels (such as Kimwipes®, Kimberly-Clark Worldwide, Inc.), isopropanol in a squirt bottle, high-efficiency particulate air (HEPA) vacuum, plastic zip-top bag, and two fine, soft-bristle nylon brushes: one flat nylon brush, such as an inexpensive toothbrush, and one round brush suitable for cleaning the interior of tubing. This procedure should be performed in a negatively pressurized hood, and gloves, goggles, and a procedure mask should be worn.

Step 1: Disconnect SAG airflow and power instrument off. Disconnect power cord. Disconnect any tubing on the outlet of the SAG. Remove SAG to a fume hood and ensure all tools and materials are on hand.

Step 2: Remove the plexiglass cover from the top of the SAG. Remove the funnel and clean it thoroughly with the HEPA vacuum and isopropanol. Set the funnel aside on a lint-free disposable towel.

Step 3 (Figure C.1):

(a) Remove the ground wire.

(b) Disconnect the nozzle by first pressing the black collar into the metal assembly and gently pulling out the yellow air hose.

(c) Loosen the T5 screw and lift the nozzle up and out of the SAG. Set aside on a wipe.

(d) Remove the dosing ring (DR) by opening the cantilever spring and lifting the DR off its tracks. Set the DR aside with the nozzle.

Step 4 (Figure C.2): Remove thumb screws on rear of instrument and remove back cover.

Step 5 (Figure C.3):

(a) Disconnect electrical connections to reservoir.

(b) While gripping the reservoir, carefully loosen the thumbscrew that holds the reservoir in place. Remove reservoir.

Step 6 (Figure C.4(a) and (b)): Unused simulant can be emptied into a glass petri dish to be baked out. Do not mix used simulant with fresh until it has been baked.

Step 7: Using the HEPA vacuum, remove any simulant left in the reservoir.

Step 8 (Figure C.5): Clean the reservoir with isopropanol and a lint-free wipe. Set aside.

Step 9 (Figure C.6): Using the HEPA vacuum, vacuum simulant from the lead screw assembly. Vacuum any simulant that falls to the floor of the SAG. Use the nylon brush and remove any stubborn simulant, then vacuum again.

Step 10 (Figure C.7): Loosen the thumb screw that holds the lead screw assembly in place. Lift entire lead screw assembly out of SAG, taking care with the electrical connection that is attached. Separate the lead screw assembly from the height adjustment. Set on the counter and vacuum lead screw assembly thoroughly, taking care not to damage the spring or allow stray simulant. Follow up with the nylon brush, and alternate between brushing and vacuuming until no simulant remains.

Step 11: Vacuum the height adjustment mechanism and follow up with the round brush. Alternate until no simulant remains.

Step 12: Vacuum the nozzle and follow up with the nylon brushes (both may be needed to thoroughly clean). Alternate until no simulant remains.

Step 13: Thoroughly vacuum the SAG until no more simulant remains.

Step 14: Follow the disassembly steps in reverse to reconstruct the SAG.

Step 15: Place all laboratory wipes in the zip-top bag, seal, and discard.

The SAG is now ready for new simulant. The SAG manual gives procedures for loading simulant using the funnel.

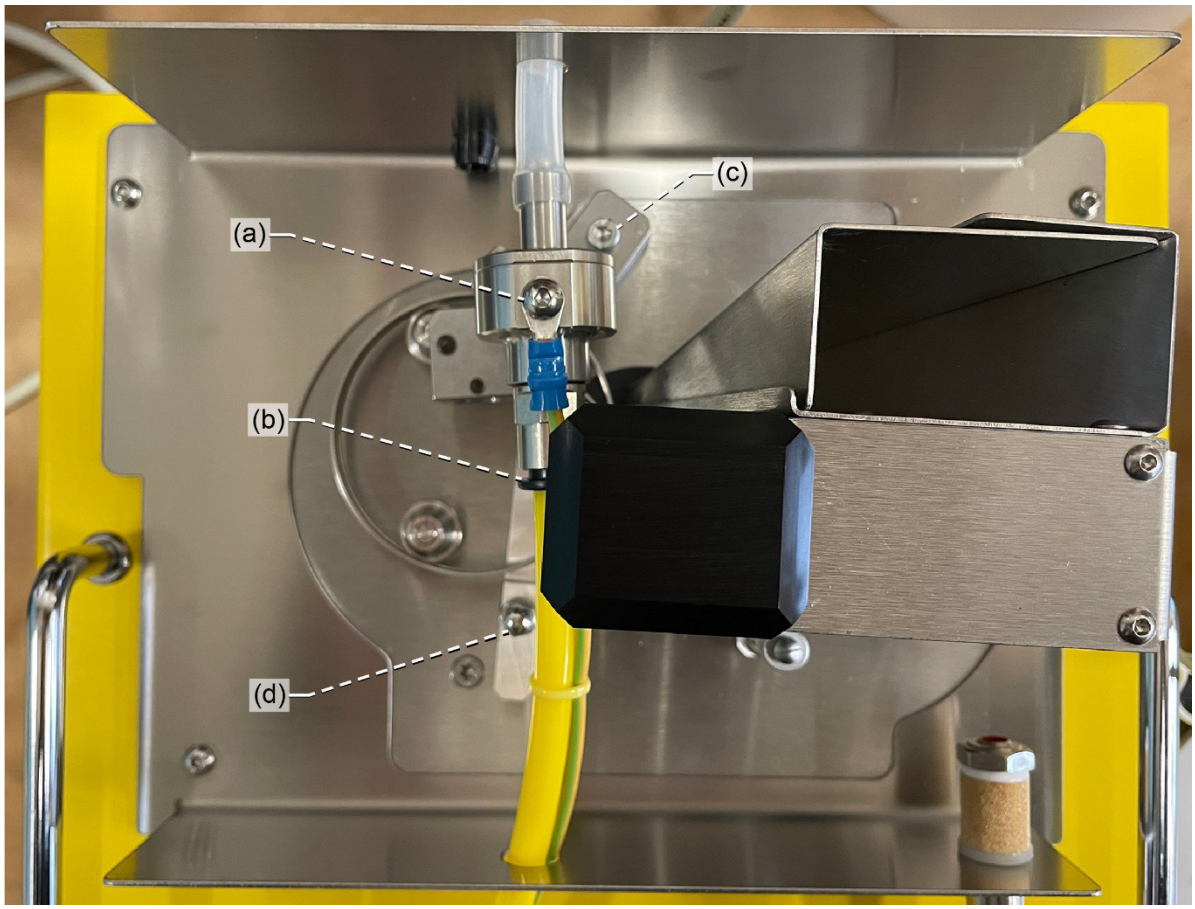

Figure C.1.—Detail of Step 3. (a) Ground wire. (b) Nozzle collar. (c) T5 screw. (d) Cantilever spring.

Figure C.2.—Detail of Step 4 showing thumb screws.

Figure C.3.—Detail of Step 5. (a) Electrical connections to reservoir. (b) Reservoir.

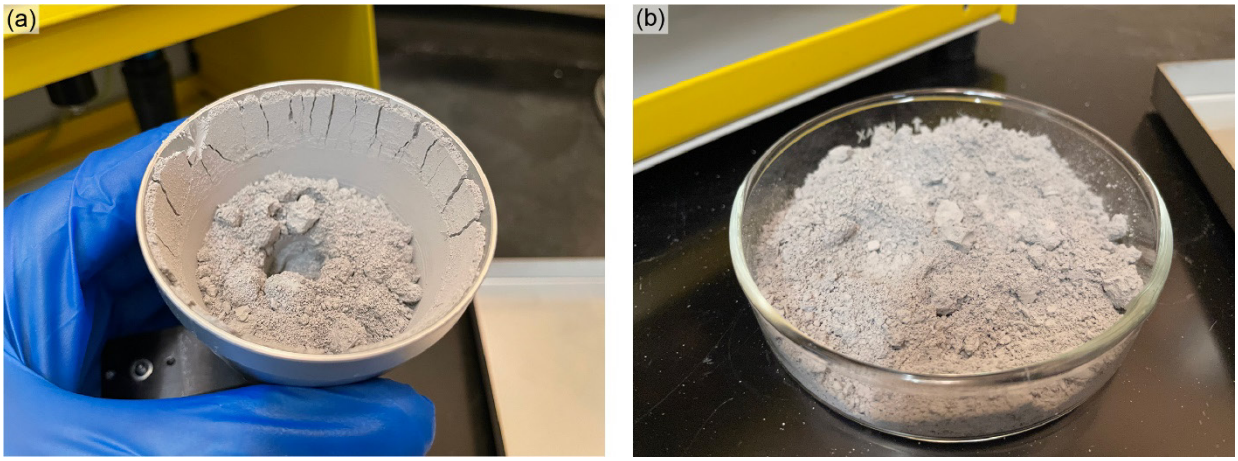

Figure C.4.—Detail of Step 6. (a) Dust in SAG reservoir after experiments. (b) Dust emptied into glass petri dish for drying.

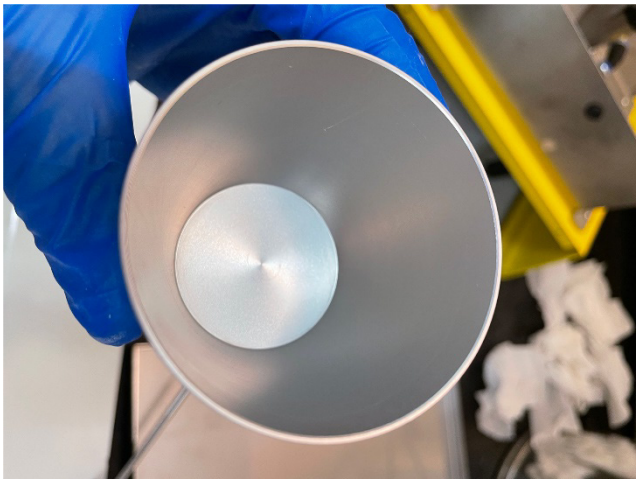

Figure C.5.—Detail of Step 8 showing clean reservoir.

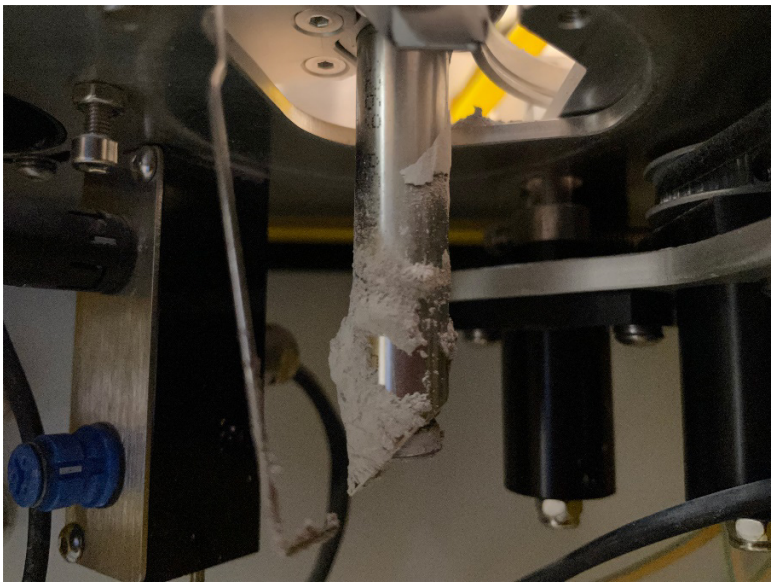

Figure C.6.—Detail of Step 9 showing simulant on lead screw assembly.

Figure C.7.—Detail of Step 10 showing thumb screw for removing lead screw assembly.

Appendix D.—DB15 Connector Pinout

TABLE D.1.—LIST OF CONNECTIONS BETWEEN DB15 CONNECTOR AND NATIONAL INSTRUMENTS USB–6008 DATA ACQUISITION CARD

DB15 pin no.	Connection name	Connection type	USB–6008 pin name
1	Actual dosing ring speed	Analog input	AI0
2	Dosing ring setpoint	Analog output	AO0
3	Reservoir rotation setpoint	Analog output	AO1
4	+5V	Power	+5V
5	Common pin for 6 to 8	Power	+5V
6	Dosing ring on/off	Digital output	P0.0
7	Reservoir rotation on/off	Digital output	P0.1
8	Airflow on/off	Digital output	P0.2
9 to 13	Ground	Power	Ground
14	Error– (Ground)	Power	Ground
15	Error+	Digital input	P0.3

References

1. National Aeronautics and Space Administration: Classifications and Requirements for Testing Systems and Hardware to be Exposed to Dust in Planetary Environments. NASA–STD–1008, 2021.
2. DeCarlo, Peter F., et al.: Particle Morphology and Density Characterization by Combined Mobility and Aerodynamic Diameter Measurements. Part 1: Theory. Aerosol Sci. Technol., vol. 38, no. 12, 2004, pp. 1185–1205.
3. National Aeronautics and Space Administration: NASA Space Flight Human System Standard Volume 2: Human Factors, Habitability, and Environmental Health. NASA–STD–3001, Vol. 2, Rev. C, 2022.
4. Vidwans, Abhay, et al.: Size and Charge Distribution Characteristics of Fine and Ultrafine Particles in Simulated Lunar Dust: Relevance to Lunar Missions and Exploration. Planet. Space Sci., vol. 210, no. 105392, 2022.
5. Colorado School of Mines: Planetary Simulant Database. 2021. https://simulantdb.com/ Accessed Oct. 4, 2022.
6. Baron, P.A.; and Willeke, K., eds.: Gas and Particle Motion. Aerosol Measurement: Principles, Techniques, and Applications, Second ed., John Wiley & Sons, New York, NY, 2001, pp. 61–82.
7. Froyd, Karl D., et al.: A New Method to Quantify Mineral Dust and Other Aerosol Species From Aircraft Platforms Using Single-Particle Mass Spectrometry. Atmos. Meas. Tech., vol. 12, 2019, pp. 6209–6239.
8. Friedlander, S.K.: Smoke, Dust, and Haze: Fundamentals of Aerosol Dynamics. Oxford University Press, New York, NY, 2000.
9. Wang, Xiaoliang, et al.: A Novel Optical Instrument for Estimating Size Segregated Aerosol Mass Concentration in Real Time. Aerosol Sci. Technol., vol. 43, no. 9, 2009, pp. 939–950.
10. TSI Incorporated: DustTrak™ DRX Aerosol Monitor Theory of Operation. Application note EXPMN–002, 2012.
11. Wang, Xiaoliang, et al.: Characterization of Smoke for Spacecraft Safety. J. Aerosol Sci., vol. 136, 2019.
12. Powder Technology, Inc.: Arizona Test Dust (ISO 12103–1 A1 Test Dust). Safety Data Sheet, 2016. https://www.powdertechnologyinc.com/wp-content/uploads/2012/08/SDS.01.Arizona-Test-Dust.4-Feb-2016.pdf Accessed Oct. 4, 2022.
13. Exolith Lab: LHS–1 Lunar Highlands Simulant. Safety Data Sheet, 2015. https://cdn.shopify.com/s/files/1/0398/9268/0862/files/LHS-1_SDS.pdf?v=1593619848 Accessed Oct. 4, 2022.
14. Meier, Reto, et al.: Differences in Indoor Versus Outdoor Concentrations of Ultrafine Particles, $PM_{2.5}$, $PM_{absorbance}$ and NO_2 in Swiss Homes. J. Expo. Sci. Environ. Epidemiol., vol. 25, 2015, pp. 499–505.
15. California Air Resources Board: Standard Operating Procedure for Organic and Elemental Carbon Analysis of Exposed Quartz Microfiber Filters. MLD065, Rev. 2.0, 2018.
16. Sumlin, Benjamin J.; and Meyer, Marit E.: A Ground Testing Program to Verify Lunar Dust-Tolerant Hardware for the Artemis Mission. ICES–2021–433, 2021.
17. Ziegler, J.G.; and Nichols, N.B.: Optimum Settings for Automatic Controllers. J. Dyn. Sys., Meas., Control, vol. 115, no. 2B, 1993, pp. 220–222.
18. Haugen, Finn: Comparing PI Tuning Methods in a Real Benchmark Temperature Control System. Model. Identif. Control, vol. 31, no. 3, 2010, pp. 79–91.